

Synthesis and optical investigations of low molecular weight alkoxy-substituted poly(*p*-phenylenevinylene)s

Francesco Babudri,^a Stefania R. Cicco,^b Luca Chiavarone,^c Gianluca M. Farinola,^b Linda C. Lopez,^b Francesco Naso^{*a} and Gaetano Scamarcio^c

^aCentro CNR di Studio sulle Metodologie Innovative di Sintesi Organiche, Dipartimento di Chimica, Università degli Studi di Bari, via Amendola 173, 70126 Bari, Italy. Fax: 0039 080 5442924; E-mail: naso@area.ba.cnr.it

^bDipartimento di Chimica, Università degli Studi di Bari, via Orabona 4, 70126 Bari, Italy

^cINFM – Dipartimento Interateneo di Fisica, Università degli Studi di Bari, via Amendola 173, 70126 Bari, Italy

Received 13th December 1999, Accepted 17th April 2000
Published on the Web 8th June 2000

Low molecular weight poly(2,5-dialkoxy-1,4-phenylenevinylene) polymers with branched, macrocyclic, and cyclic polyetheral alkoxy chains have been prepared by Stille cross-coupling reaction between suitable 2,5-dialkoxy-1,4-diiodobenzenes and (*E*)-1,2-bis(tributylstannyl)ethene. Spectral line narrowing in solution and film under high pulsed excitation intensity is reported. The measurement of the photoluminescence efficiency in film is carried out. The PPV with macrocyclic alkoxy substitution shows higher efficiency but lower damage threshold than the PPV derivative with open alkoxy chains. The potential of these materials in electroluminescent devices is discussed.

Introduction

In recent years, new perspectives in the field of semiconductor devices have been disclosed by the possibility of employing conjugated polymers as active elements.¹ The optical and electronic properties of semiconductors, associated with the processing advantages and mechanical properties of polymers, make these new materials very attractive in the fabrication of light-emitting diodes² and other categories that characterise the field of photonic devices. In particular, the observation of electroluminescence in poly(1,4-phenylenevinylene) (PPV),³ the simplest and cheapest poly(arylenevinylene) polymer, has boosted development of new materials structurally related to the underivatized PPV,⁴ with the aim of modulating the optical and electrooptical properties. A rapidly emerging area of more recent interest for applications of these conjugated polymers is represented by their use as organic semiconductor lasers.⁵

It is also worth noting that oligomers may present similar electrooptical properties to the corresponding longer chain systems.^{6,7} In particular, amplified spontaneous emission, the main factor for obtaining laser action, has been reported in PPV oligomer thin film, with an emission threshold comparable with those noticed in conjugated polymer thin film.⁸ Within the framework of our studies dealing with the application of organometallic reagents to the synthesis of stereodefined conjugated polyenes and polymers⁹ we have recently reported the synthesis of poly(2,5-pentyloxy-1,4-phenylenevinylene) by the Stille cross-coupling reaction.^{9a} This organometallic procedure affords low molecular weight polymers,^{9a,10} and it is particularly attractive in view of the large number of materials which could be obtained and then subjected to interesting structure–properties relationship studies.

In this work, we report the application of our procedure to the synthesis of three low molecular weight PPV polymers with open branched, bridged macrocyclic or cyclic polyetheral alkoxy chains, together with an investigation of their optical properties. A comparison of light emission under high laser excitation between solutions and films has been performed.

Results and discussion

1. Synthesis of polymers

The synthesis of polymers **1a–1c** (Fig. 1) was performed by cross-coupling reaction of (*E*)-1,2-bis(tributylstannyl)ethene **4** with diiododerivatives **3a–3c** in refluxing benzene in the presence of tetrakis(triphenylphosphine)palladium(0) as the catalyst (Scheme 1). Diiodo aromatic derivatives **3a–3c** were prepared by iodination reaction of the corresponding hydroquinone diethers **2a–2c** with HIO₃–I₂ (Scheme 1).¹¹ Diethers **2a**¹² and **2b**¹³ were prepared according to reported procedures. The cyclic polyether **2c** was obtained as shown in Scheme 2, starting from hydroquinone and the dibromo derivative **5**,¹⁴ prepared from the corresponding tetraethylene glycol by bromination with PBr₃. Molecular weights, reported in Table 1, were determined by gel-permeation chromatography (GPC) with uniform polystyrene standards. Actually the

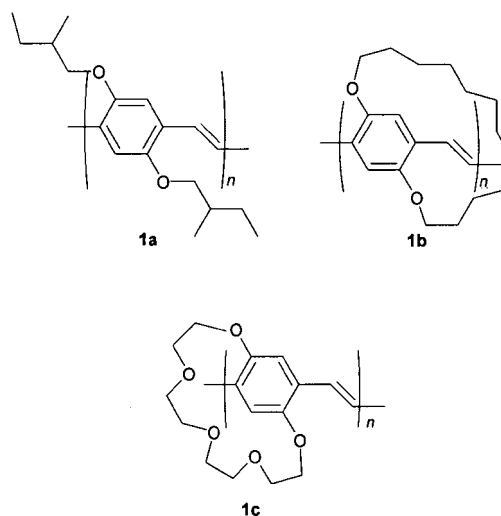
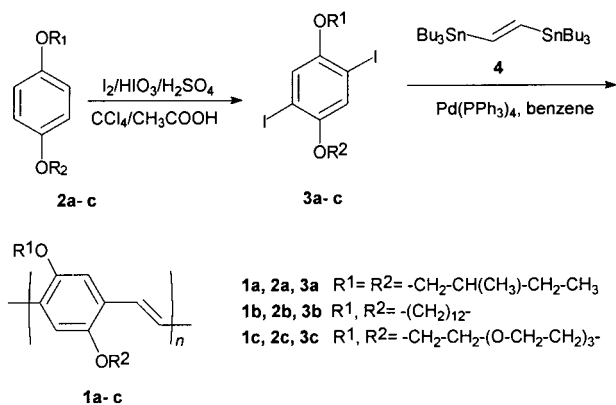
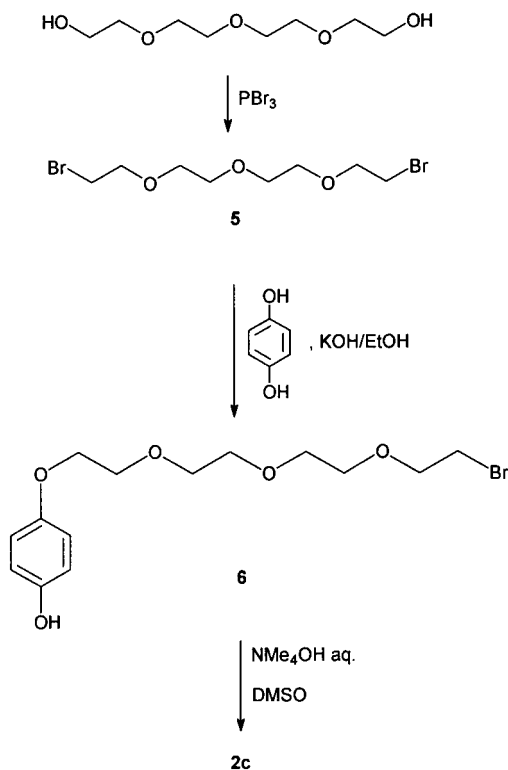


Fig. 1 Structures of polymers **1a–1c**.



Scheme 1 Synthesis of PPV derivatives **1a–1c**.



Scheme 2 Synthesis of compound **2c**.

number-averaged molecular weights (M_n) of rigid rod polymers are usually overestimated when determined using the randomly coiled polystyrene standards.¹⁵ Nevertheless, the GPC recorded M_n values could be used for determining a trend in degrees of polymerization when we consider the structurally similar polymers **1a–1c**. Thus polymer **1a** and **1b**, although their M_n values are not absolute, have very close degrees of polymerization, whereas **1c** is a shorter chain oligomer than **1a** and **1b**.

When considering these low molecular weight polymers, the important question about the nature of the terminal groups arises, which may in principle influence their photophysical

properties. In order to ascertain the nature of the chain terminations we have performed an XPS analysis of **1a–1c** for evaluating the tin and iodine contents. This analysis revealed low values of atomic concentrations of both the elements (under 0.5%), very near to the detection threshold. Therefore, hydrogen atoms are the most probable end groups of **1a–1c**. It is likely that reductive dehalogenation and destannylation steps may occur as side reactions during the polymerization process, and the low molecular weight of the polymers prepared this way may be ascribed also to the loss of the reactive groups at the ends of relatively short chains.

2. Optical absorption and low and high excitation intensity emission spectra of solutions

Fig. 2 shows the absorption and photoluminescence spectra of polymers **1a–1c**. All the spectra of Fig. 2a show a broad band ascribed to the π - π^* transition. The corresponding peak wavelengths (λ_{max}) are reported in Table 2, together with the HOMO–LUMO energy gap E_g , evaluated from the absorption spectra as the maximum of the first derivative with respect to energy.¹ The results of Table 2 show the following relation: E_g (**1c**) > E_g (**1b**) > E_g (**1a**). In polymers **1a** and **1b**, the inductive and mesomeric effects of substituents on the conjugated backbone can be considered constant, because of the identical conjugated structure and position of substituents and the similar nature of the latter. Their degrees of polymerization (Table 1) are also similar. Therefore, the observed trend in E_g values can be ascribed to a reduction of the conjugation length, associated with the twist of the phenyl rings out of the vinylene plane. For the polymer **1c**, the effect of a lower degree of polymerization may play a significant role in enhancing the energy gap value. This is confirmed by the observed ~ 100 meV increase of E_g , associated with a reduction from 7 to 5 of the monomeric units in PPV oligomers.¹⁶

The cw photoluminescence (PL) spectra are shown in Fig. 2b. The PL spectra are redshifted with respect to the

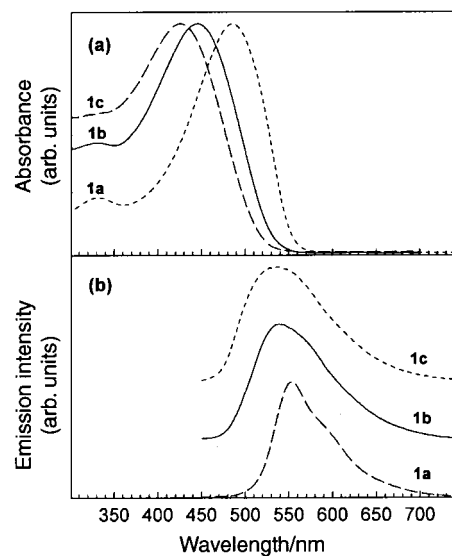


Fig. 2 Absorption (a) and photoluminescence (b) spectra of the **1a**, **1b** and **1c** polymers in CHCl_3 solution.

Table 1 Molecular weights of polymers **1a–1c**

Polymer	$M_n^{a,b}/\text{Da}$	$M_w^{a,c}/\text{Da}$	M_w/M_n	N_n^d
1a	2260	3180	1.4	8.2
1b	2230	3180	1.4	7.4
1c	1330	1880	1.4	4.6

^aDetermined by gel-permeation chromatography (GPC) with uniform polystyrene standards and THF as a solvent. ^bNumber-averaged molecular weight. ^cWeight-averaged molecular weight. ^dNumber averaged degree of polymerization.

Table 2 Spectroscopic data of the **1a–1c** polymers in solution and film

Polymer	$\lambda_{\text{max}}^{\text{ABS}}/\text{nm}^a$	$\lambda_{\text{max}}^{\text{PL}}/\text{nm}^b$	E_g/eV^c	$\lambda_{\text{max}}^{\text{ASE}}/\text{nm}^d$	FWHM/nm ^e	Φ_{PL} (%)
1a	485	553	2.33	593	8	5.9 ± 0.6
1b	446	540	2.51	570	10	15–24 ± 2
1c	425	536	2.58	551	20	—
MEH-PPV	—	—	—	—	—	10–15 ± 1 ²⁴

^aMaximum absorption wavelength. ^bMaximum emission wavelength. ^cValue of the π - π^* energy gap evaluated from the absorption spectra of Fig. 1a. ^dPeak wavelength of the narrow emission under high pulsed excitation intensity. ^eFull width half maximum band of the narrow emission under high pulsed excitation intensity.

absorption ones (Stokes shift) owing to the higher degree of coplanarity of the conjugated backbone in the excited state due to the aromatic to quinoid conversion.¹⁷ This Stokes shift is beneficial in reducing self-absorption effects and can be exploited to investigate optical gain phenomena in organic materials.⁵ This is shown in Fig. 3, in which the emission spectra of polymers **1a–1c** under pulsed high excitation intensity are reported. Above a given excitation intensity, the emission becomes directional and the broad band spectrum collapses in a narrow spectral line whose peak position ($\lambda_{\text{max}}^{\text{ASE}}$) and full width half maximum (FWHM) are reported in Table 2. In the insets of Fig. 3 the FWHM and the emission peak intensity are reported as a function of the excitation intensity I_{exc} . In the case of **1a**, for $I_{\text{exc}} > 1.2 \text{ mJ cm}^{-2}$ a narrow spectral line at 593 nm emerges from the broad band which collapses into the narrow spectral line with a FWHM of 8 nm for $I_{\text{exc}} > 1.9 \text{ mJ cm}^{-2}$. At these values of I_{exc} , the linear fit reported in the inset of Fig. 3a shows that the emission peak intensity varies exponentially with respect to I_{exc} . This indicates amplified spontaneous emission (ASE),¹⁸ *i.e.*, light amplification by stimulated emission after a single pass through the gain

medium, as the mechanism responsible for the spectral line narrowing. The behaviour of **1b** is similar to that of **1a**, but the amplification is less efficient. Indeed a narrow spectral line is obtained with higher excitation levels ($I_{\text{exc}} > 3.2 \text{ mJ cm}^{-2}$) and the emission peak intensity is an order of magnitude smaller with the same value of I_{exc} , in spite of the larger concentration (2.0 mg ml^{-1} in CHCl_3 with respect to 1.3 mg ml^{-1} in CHCl_3). Moreover, the superlinear trend of the peak emission intensity is not exponential, showing that the amplification of the spontaneous emission is a less steady phenomenon with respect to **1a**. This behaviour is enhanced in **1c** (2.1 mg ml^{-1} in CHCl_3) where the FWHM does not change abruptly and a slight superlinear increase of the peak intensity is evident only for $I_{\text{exc}} > 10 \text{ mJ cm}^{-2}$. For this reason we have restricted the study of the emission properties in the solid state to **1a** and **1b** polymers.

3. Low excitation intensity film emission: photoluminescence efficiency

The photoluminescence (PL) efficiency in the solid state is a fundamental parameter to evaluate the possibility of using these polymers in electroluminescent devices. The results obtained with the procedure illustrated in the Experimental section are reported in Table 2. The polymer **1a** is approximately three times less efficient than **1b**. The greater efficiency of **1b** is attributed to the reduction of the interaction between adjacent chains due to the bridged structure of the alkoxy substitution.¹⁹ It is worth noting that the PL efficiency is larger in **1b** than in MEH-PPV, which is the prototype polymer for the fabrication of light emitting diodes based on dialkoxy-PPV. Furthermore, the PL efficiency ratio is maintained in electroluminescence. Fig. 4 shows the current–voltage (I – V curve) and the optical power as a function of current (L – I curve) characteristics for an ITO/**1b**/Al light emitting diode (LED). Yellow light becomes visible to the eye above 17.4 V. From the slope of the L – I characteristics we extract an external electroluminescence efficiency $\eta = 0.015\%$, defined as the number of emitted photons per injected carrier. Significantly, for a similar LED with MEH-PPV, a lower value of $\eta = 0.008\%$ is reported.²⁰

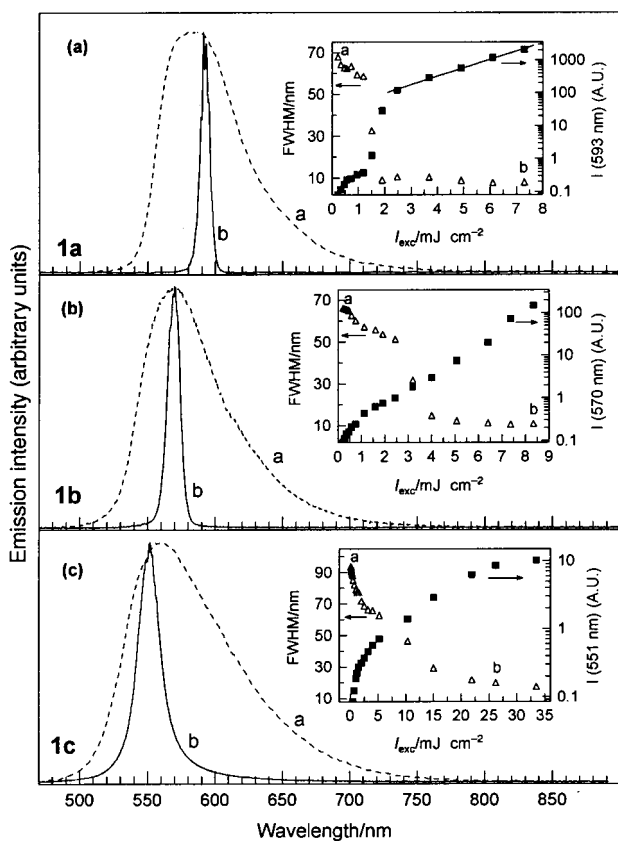


Fig. 3 Normalised luminescence spectra of **1a–1c** polymers in CHCl_3 solution at pulsed excitation intensities below (dashed line) and above (solid line) the threshold for the observation of the spectral line narrowing process. In the insets the FWHM and the emission peak intensity as a function of the excitation intensity are reported.

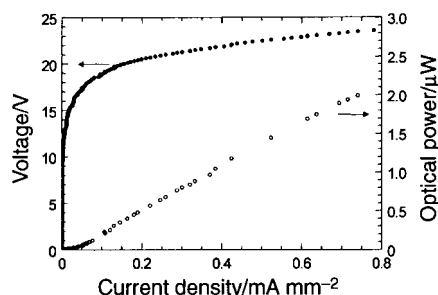


Fig. 4 Current–voltage and power–current characteristics of an ITO/**1b**/Al LED.

4. High excitation intensity film emission: spectral line narrowing

The emission spectra of the **1a** and **1b** polymer films under high pulsed excitation intensity are reported in Fig. 5. As in the solutions, above a given excitation intensity spectral narrowing of the emission band occurs. The narrow band is distinguished for intensities above 46 mJ cm^{-2} in **1a** and 21 mJ cm^{-2} in **1b**. As for the solution, in **1b** films the narrow band is centred at 570 nm and the observation of the spectral line narrowing is more critical than in **1a** films. In fact, the **1b** film is damaged after few excitation pulses, although measurements were performed under vacuum. The lower threshold can be ascribed both to a better uniformity of **1b** films, which guarantees the waveguide effect of the light, and to the much higher PL efficiency. In solution, PL efficiencies are comparable,¹⁹ explaining the higher threshold observed for **1b**.

Conclusion

In conclusion, we have employed the Stille methodology for the synthesis of low molecular weight alkoxy PPV derivatives with branched **1a** and bridged **1b**, **1c** substituents. The investigation of their optical properties represents further evidence that oligomers may be used beside high molecular weight materials in optical and electrooptical applications.

We have correlated the optical properties with the substituent structure, demonstrating that bridged macrocyclic functionalization is beneficial for increasing the emission efficiency of dialkoxy-PPVs and may have useful applications for LEDs. On the other hand, open chain dialkoxy substitution appears more suitable for laser action.

Summing up, the validity of our approach appears clearly demonstrated. Indeed, we have applied one of the most versatile carbon-carbon bond forming reactions to the production of stereodefined PPV systems. After our work, the possibility of using such a process appears well established and this opens a highway to such systems. Furthermore, we have found that the materials obtained in a straightforward and operationally simple manner, in spite of their low molecular weight, present photophysical properties of special interest whose fine tuning, in principle, is made possible by the versatility of the synthetic procedure set up.

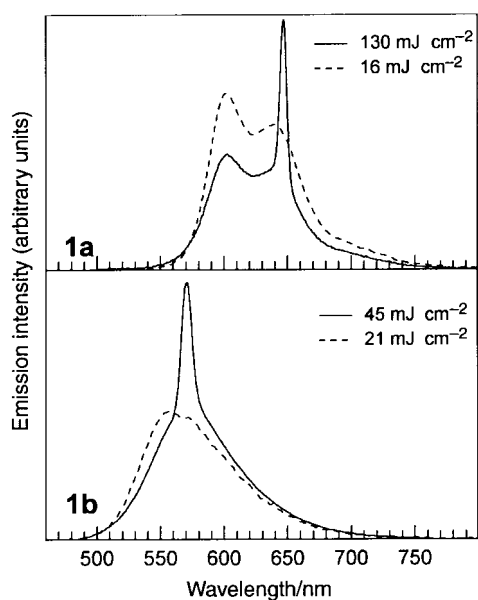


Fig. 5 Emission spectra of **1a** and **1b** polymer films at pulsed excitation intensities below (dashed line) and above (solid line) the threshold for the observation of the spectral line narrowing process.

Experimental

General

Macherey-Nagel silica gel 60 (particle size 0.040–0.063 mm) for flash chromatography and Macherey-Nagel aluminium sheets with silica gel 60 F₂₅₄ for TLC were used. GC/mass spectrometry analyses were performed on a Hewlett-Packard 5890 gas chromatograph equipped with a HP-1 capillary column and HP MSD 5970B mass selective detector. ¹H NMR and ¹³C NMR spectra were recorded on a Bruker AM 500 spectrometer at 500 MHz and at 125.7 MHz respectively, or on a Varian XL 200 at 200 MHz and at 50.7 MHz respectively using the residual CHCl₃ signal at δ 7.24 ppm as the standard for the ¹H data and the triplet centred at δ 77.00 for the ¹³C data. FT-IR spectra were registered on a Perkin-Elmer 1710 spectrometer on KBr pellets. Molecular weights were determined with a Hewlett-Packard HP 1050 liquid chromatograph instrument using THF as a solvent and a Plgel 5 μ Mixed-D 300 \times 7.5 mm column. Diethers **2a**,¹² **2b**,¹³ dibromide **5**,¹⁴ and the monomer **4**²¹ were prepared as reported. Tetrakis(triphenylphosphine)palladium(0) was a commercial product. Benzene was distilled immediately prior to use from sodium-benzophenone in a nitrogen atmosphere. Reactions sensitive to oxygen and moisture were conducted under a nitrogen atmosphere. Films with thickness larger than 200 nm were formed by spin coating on quartz substrates.

Synthesis

1,4-Diiodo-2,5-bis(2-methylbutoxy)benzene (3a). 1,4-Bis(2-methylbutoxy)benzene **2a** (5.45 g, 21.6 mmol), I₂ (4.88 g, 19.2 mmol), HIO₃ (4.60 g, 26.2 mmol), and H₂SO₄ (30% aqueous solution, 6 mL) in CCl₄ (13 mL) and acetic acid (28 mL) were heated at 75 °C overnight under stirring. The resulting mixture was cooled, diluted with water (50 mL) and extracted with ethyl acetate (3 \times 30 mL). The organic phase was washed with an aqueous solution of sodium thiosulfate (10%, 50 mL) and water (50 mL), dried over anhydrous sodium sulfate, and the solvent evaporated at reduced pressure. The crude product was crystallised twice from ethanol, and 5.69 g (52% yield) of white crystals were obtained (mp 74–76.5 °C). ¹H NMR (500 MHz, CDCl₃): δ 0.94 (t, J =7.5 Hz, 6H), 1.04 (d, J =6.8 Hz, 6H), 1.25–1.35 (m, 2H), 1.54–1.64 (m, 2H), 1.83–1.91 (m, 2H), 3.69 (dd, J =8.7, 6.4 Hz, 2H), 3.77 (dd, J =8.7, 5.7 Hz, 2H), 7.11 (s, 2H) ppm. GC/MS (70 eV) m/z (%) 502 (M⁺, 4), 432 (2), 362 (100), 304 (4), 236 (2), 207 (4), 110 (12), 43 (47). C₁₆H₂₄O₂I₂: Calcd C, 38.27; H, 4.82; Found C, 38.57; H, 4.65%.

17,19-Diiodo-2,15-dioxabicyclo[14.2.2]jicosa-1(19),16(20),17-triene (3b). The synthesis of this compound was performed following the same procedure reported for compound **3a**, starting from 2,15-dioxabicyclo[14.2.2]jicosa-1(19),16(20),17-triene **2b** (1.64 g, 5.9 mmol), I₂ (1.36 g, 5.3 mmol), HIO₃ (1.26 g, 7.2 mmol), and H₂SO₄ (30% aqueous solution, 1.8 mL) in CCl₄ (3 mL) and acetic acid (11 mL) at 50 °C for 5 h. The crude product was purified by crystallisation from petroleum ether. 0.97 g (31% yield) of a white solid (mp 99–102 °C) were obtained. ¹H NMR (500 MHz, CDCl₃): δ 0.94 (s, 8H), 1.02–1.12 (m, 2H), 1.14–1.23 (m, 2H), 1.24–1.41 (m, 4H), 1.54–1.63 (m, 2H), 1.68–1.78 (m, 2H), 4.19 (ddd, J =11.8, 8.3, 4.1 Hz, 2H), 4.27 (ddd, J =11.8, 6.1, 4.2 Hz, 2H), 7.23 (s, 2H) ppm. ¹³C NMR (125 MHz, CDCl₃): δ 23.95, 26.77, 27.44, 27.94, 28.51, 69.54, 87.25, 124.52, 151.78 ppm. GC/MS (70 eV) m/z (%) 528 (M⁺, 18), 362 (100), 149 (2), 135 (2), 69 (6), 55 (18), 41 (20). Anal. Calcd for C₁₈H₂₆O₂I₂: C, 40.93; H, 4.96. Found: C, 40.81; H, 4.84%.

4-(2-{2-[2-(2-Bromoethoxy)ethoxy]ethoxy}ethoxy)phenol (6). In a light stream of nitrogen, an aqueous solution of

NMe₄OH (1.1 M, 32 mL, 35.2 mmol) was added dropwise to a stirred solution of hydroquinone (3.89 g, 35.3 mmol) and dibromide **5** (11.30 g, 35.3 mmol) in DMF (80 mL). The resulting mixture was warmed for 6 h at 80 °C, then diluted with water (250 mL) and extracted with ethyl acetate (3 × 50 mL). The organic phase was washed with water (5 × 100 mL), dried over anhydrous sodium sulfate, and the solvent removed under reduced pressure. A thick light yellow oil was obtained (5.03 g, 41% yield). ¹H NMR (200 MHz, CDCl₃): δ 3.43–3.57 (m, 2H), 3.63–3.97 (m, 12H), 4.01–4.17 (m, 2H), 6.70 (s, 1H, OH), 6.72–6.88 (m, 4H) ppm. GC/MS (70 eV) *m/z* (%) 350 (M+2, 4), 348 (M⁺, 4), 241 (11), 239 (11), 153 (17), 151 (17), 110 (38), 109 (100), 107 (88), 81 (17), 65 (12). Anal. Calcd for C₁₄H₂₁O₅Br: C, 48.15; H, 6.06. Found: C, 47.85; H, 5.94%.

2,5,8,11,14-Pentaoxabicyclo[13.2.2]nonadeca-1(18),15(19),16-triene (2c). A solution of **6** (2.51 g, 7.2 mmol) in DMSO (36 mL) and NMe₄OH in water–DMSO (6.5 mL of an aqueous solution 1.1 M, 7.2 mmol, diluted with DMSO–water 80% up to 36 mL) were added dropwise at the same time to DMSO (300 mL, previously degassed by bubbling a nitrogen stream for 1 h), warmed at 80 °C under a vigorous stirring. The slow addition required about 4 h. The resulting mixture was cooled to room temperature and stirred overnight. Most of the solvent was then removed by distillation under reduced pressure (80 Torr, 85–90 °C). When the volume of the residue of the distillation was reduced to about 30 mL, the distillation was stopped, and water (200 mL) was added. The resulting mixture was extracted with dichloromethane (3 × 50 mL), the organic phase washed with water (3 × 100 mL), and dried over anhydrous sodium sulfate. The solvent was then removed under reduced pressure. The crude product was purified by flash chromatography (silica gel, ethyl acetate–petroleum ether 70:30). A yellow oil was obtained (0.51 g, 26% yield). ¹H NMR (200 MHz, CDCl₃): δ 3.20–3.28 (m, 4H), 3.32–3.40 (m, 4H), 3.66–3.74 (m, 4H), 4.22–4.30 (m, 4H), 6.92 (s, 4H) ppm. ¹³C NMR (50 MHz, CDCl₃): δ 68.66, 70.25, 70.43, 72.32, 118.06, 153.71 ppm. GC/MS (70 eV) *m/z* (%) 268 (M⁺, 100), 180 (2), 136 (10), 121 (5), 110 (24), 109 (5), 108 (11), 82 (13), 80 (9), 73 (15), 64 (10). Anal. Calcd for C₁₄H₂₀O₅: C, 62.67; H, 7.51. Found: C, 62.58; H, 7.32%.

16,18-Diiodo-2,5,8,11,14-pentaoxabicyclo[13.2.2]nonadeca-1(18),15(19),16-triene (3c). The synthesis of this compound was performed following the same procedure reported for compound **3a**, starting from **2c** (0.32 g, 1.2 mmol), I₂ (0.28 g, 1.1 mmol), HIO₃ (0.13 g, 0.7 mmol), and H₂SO₄ (30% aqueous solution, 0.4 mL) in CCl₄ (0.5 mL) and acetic acid (2 mL) at 50 °C for 4 h. The crude product was purified by flash chromatography (silica gel, ethyl acetate–petroleum ether 70:30).

A white solid was obtained (mp 128–131 °C, 0.29 g, 46% yield). ¹H NMR (500 MHz, CDCl₃): δ 3.26–3.32 (m, 2H), 3.34–3.43 (m, 6H), 3.68–3.73 (m, 2H), 3.78–3.84 (m, 2H), 4.20–4.26 (m, 2H), 4.39–4.46 (m, 2H), 7.33 (s, 2H) ppm. ¹³C NMR (125 MHz, CDCl₃): δ 70.60, 71.31, 71.34, 72.28, 88.68, 126.67, 154.39 ppm. GC/MS (70 eV) *m/z* (%) 520 (M⁺, 100), 360 (17), 233 (9), 205 (15), 134 (12), 106 (10), 73 (28), 53 (25), 45 (63), 43 (71). Anal. Calcd for C₁₄H₁₈O₅I₂: C, 32.33; H, 3.49. Found: C, 31.78; H, 3.43%.

Poly[2,5-bis(2-methylbutoxy)-1,4-phenylenevinylene] (1a). A mixture of 1,4-diiodo-2,5-bis(2-methylbutoxy)benzene **3a** (1.00 g, 2.0 mmol), (*E*)-1,2-bis(*n*-tributylstannyl)ethene **4** (1.03 g, 2.0 mmol) and tetrakis(triphenylphosphine)palladium(0) (0.069 g, 0.06 mmol), in anhydrous benzene (30 mL) was refluxed in a nitrogen atmosphere. After 3 days a dark red precipitate slowly separated from the reaction mixture. After 5 days the mixture was cooled to room temperature, the solvent

was evaporated under reduced pressure, and the residue was diluted with water and extracted with CH₂Cl₂ (3 × 50 mL). The crude polymer obtained from evaporation of the solvent was washed thrice with hexane. The solid was recovered after each washing by centrifugation. Low molecular weight fractions were eliminated by extraction in a Soxhlet apparatus with ethanol for 24 hours, followed by a second extraction with CHCl₃. After evaporation of the solvent, the dark red powder obtained (0.33 g, 60% yield) was dried at 90 °C and 10⁻² mbar. The polymer is soluble in CH₂Cl₂ and CHCl₃, insoluble in ethanol. IR (KBr) ν 3062, 2960, 2922, 1508, 1459, 1421, 1257, 1202, 1103, 1046, 801 cm⁻¹. ¹H NMR (500 MHz, CDCl₃): δ 0.94–1.02 (m, 6H), 1.03–1.17 (m, 6H), 1.28–1.43 (m, 2H), 1.57–1.72 (m, 2H), 1.89–2.04 (m, 2H), 3.75–3.95 (m, 4H), 7.16 (br s, 2H), 7.51 (br s, 2H) ppm. ¹³C NMR (125 MHz, CDCl₃): δ 11.50, 16.85, 26.42, 35.09, 74.28, 110.05, 122.70, 127.48, 151.15 ppm. Anal. Calcd for (C₁₈H₂₆O₂)_n: C, 78.78; H, 9.55. Found: C, 80.73; H, 9.03%.

Poly[2,15-dioxabicyclo[14.2.2]jicosa-1(19),16(20),17-trien-17,19-ylenevinylene] (1b). This polymer was prepared following the procedure above described for the polymer **1a**, starting from 17,19-diiodo-2,15-dioxabicyclo[14.2.2]jicosa-1(19),16(20),17-triene **3b** (0.25 g, 0.47 mmol), (*E*)-1,2-bis(*n*-tributylstannyl)ethene **4** (0.29 g, 0.48 mmol) and tetrakis(triphenylphosphine)palladium(0) (0.017 g, 0.015 mmol), in anhydrous benzene (20 mL) for 7 days. After the workup above described for the polymer **1a**, a dark red solid was obtained (0.082 g, 58% yield). IR (KBr) ν 3054, 2923, 2851, 1592, 1494, 1460, 1417, 1245, 1186, 1049, 999, 970, 874, 691 cm⁻¹. ¹H NMR (500 MHz, CDCl₃): δ 0.70–2.10 (m, 20H), 3.90–4.10 (m, 4H), 7.24 (br s, 2H), 7.5 (br s, 2H) ppm. ¹³C NMR (125 MHz, CDCl₃): δ 24.16, 27.43, 27.93, 28.41, 28.54, 68.90, 112.66, 123.23, 128.62, 150.26 ppm. Anal. Calcd for (C₂₀H₂₈O₂)_n: C, 79.95; H, 9.39. Found: C, 81.66; H, 9.83%.

Poly[2,5,8,11,14-pentaoxabicyclo[13.2.2]nonadeca-1(18),15(19),16-trien-16,18-ylenevinylene] (1c). This polymer was prepared following the procedure above described for the polymer **1a**, starting from 16,18-diiodo-2,5,8,11,14-pentaoxabicyclo[13.2.2]nonadeca-1(18),15(19),16-triene **3c** (0.19 g, 0.36 mmol), (*E*)-1,2-bis(*n*-tributylstannyl)ethene **4** (0.22 g, 0.36 mmol) and tetrakis(triphenylphosphine)palladium(0) (0.013 g, 0.012 mmol), in anhydrous benzene (20 mL) for 9 days. After the workup above described for the polymer **1a**, consisting of Soxhlet extraction with hexane for removing low molecular weight fractions and a second extraction with methanol, a dark red solid was obtained (0.088 g, 83% yield, mp 130–140 °C). IR (KBr) ν 2956, 2925, 2854, 1598, 1489, 1459, 1417, 1260, 1186, 1106, 1050, 948, 802 cm⁻¹. ¹H NMR (500 MHz, CDCl₃): δ 2.58–3.40 (m, 8H), 3.45–3.85 (m, 4H), 4.00–4.35 (m, 2H), 4.45–4.70 (m, 2H), 6.85–7.75 (m, 4H) ppm. ¹³C NMR (125 MHz, CDCl₃): δ 70.53, 70.84, 72.22, 114.73, 123.80, 128.59, 152.14 ppm. Anal. Calcd for (C₁₆H₂₀O₅)_n: C, 65.74; H, 6.90. Found: C, 62.51; H, 7.65%.

Optical measurements

Absorption and emission spectra. Absorption measurements were performed with a Varian DMS 100 double beam spectrometer. For cw PL spectra, the solutions were excited with the 441.6 nm line of a He–Cd ion laser. Absorption and cw PL spectra of solutions with a concentration of ~20 mg l⁻¹ were recorded in order to make negligible inter-chain interactions. PL measurements under high pulsed excitation energy were performed exciting the solutions with the output of a dye laser pumped by a 10 Hz Q-switched Nd:YAG laser providing ~10 ns pulses. The output wavelength of the dye laser was settled at the maximum absorption of the solutions and films. The pump laser beam was first expanded and then

focused onto the samples, by a cylindrical lens for obtaining a narrow rectangular excitation area (0.24×8 mm). The incidence angle was nearly 90 degrees and the emission was collected from the side of the sample. Films were kept under a vacuum of 10^{-5} mbar to prevent photooxidation and the solutions were contained in a $1 \times 0.5 \times 3$ cm cuvette. The emission was spectrally analysed by a system comprising a monochromator and a CCD detector, having a spectral resolution of 1.5 nm. All measurements were performed at room temperature.

Photoluminescence efficiency. Comparison of the emission intensity with that of a standard material gives approximate values, because the emission angular distribution is not isotropic as for the solutions, but it is strongly related to refractive index of the material and to the morphology of the film. For this reason the PL efficiencies were assessed by means of an integrating sphere which redistributes isotropically the emission of the film regardless of its angular dependence over the interior surface.

We followed the experimental procedure described by de Mello *et al.*²² The experimental set-up for the measurement is shown in Fig. 6. We used a modified Ocean Optics integrating sphere with an internal diameter of 50 mm and a sample port with a diameter of 8 mm. The samples were fixed on a Teflon support and put inside the sphere through the sample support. The films were excited with the 441.6 nm line of a He–Cd laser. The beam laser was guided into a 600 μ m optical fibre and focused onto the sample with a lens, having the optical axis forming an angle of 8 degrees with respect to the normal. Laser power was kept below 0.1 mW, with a beam diameter at the sample of 4 mm. The signal was collected with an identical fibre at 90 degrees coupled with the spectrometer. This configuration of sample excitation and collection of the signal does not require the use of a diffusive baffle to prevent direct illumination of the optical fibre. The assessment of the PL efficiency involves three steps outlined in Fig. 6. In the first configuration, the sphere is empty (Fig. 6a); this measurement allows to determine the laser light incident onto the sample. The second measurement is made with the sample placed inside the sphere and the laser light directed on the sphere wall (Fig. 6b). This configuration provides the way to evaluate the secondary emission, *i.e.* emission due to illumination of the sample by diffuse laser light. The third configuration is similar to the second one, but with the collimated laser beam directed on the sample (Fig. 6c). The corresponding measured spectra for **1a** are shown in Fig. 7. The line at 441.6 nm corresponds to the detection of the laser light and the band at longer wavelengths to the detection of the emission sample. The area under the laser profile is proportional to the unabsorbed laser photons, while the area under the band is proportional to the emitted photons. The evaluation of these areas in the three experiments gives the PL efficiency.²² It is important to stress that the area under the emission band was corrected for the re-absorption of the emitted light in the spectral range where the emission and the absorption bands overlap. This effect is

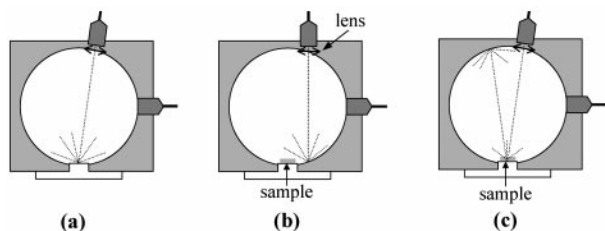


Fig. 6 Scheme of the measurement of the PL efficiency in the solid state: (a) the sphere is empty, (b) the sample is placed inside the sphere and the beam laser is incident onto the sphere wall, (c) the sample is placed inside the sphere and the beam laser is incident on the sample.

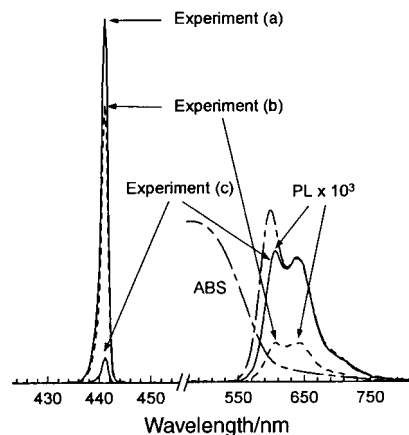


Fig. 7 Measured spectra for a film of **1a** polymer in the three configurations illustrated in Fig. 5. The PL spectra have been enlarged by a factor of 10^3 for clarity. The absorption band and the PL spectrum (short long dashed lines) taken with the sample outside the sphere are reported to display the re-absorption effect.

shown in Fig. 7. The correction was made comparing the photoluminescence spectra taken with the sample inside and outside the sphere.

Electroluminescence efficiency. Light emitting diodes have been prepared by spin-coating a 58 nm thick **1b** PPV layer onto indium-tin-oxide (ITO) coated glass from a tetrachloroethane solution. ITO glass was previously treated with an oxygen plasma in a reactive ion etching (RIE) reactor. This treatment, lowering the ratio Sn : In and increasing the oxygen concentration on the material surface,²³ leads to a lower turn-on voltage. Al top contacts of 3 mm \times 3 mm area were thermally evaporated. *I–V*, and *L–I* characteristics were measured in air at room temperature with a Hewlett-Packard HP4145B semiconductor analyser and a calibrated photodiode.

Acknowledgements

This work was financially supported by Ministero dell'Università e della Ricerca Scientifica e Tecnologica, Rome, by the University of Bari (National Project "Stereoselezione in Sintesi Organica. Metodologie ed Applicazioni"), and by Consiglio Nazionale delle Ricerche, Rome (National Project "Progetto Finalizzato Materiali Speciali per Tecnologie Avanzate II"). We are very grateful to Drs Fabio Palumbo and Ernesto Mesto of CNR Centro di Chimica dei Plasmi- Bari for the XPS analyses.

References

- 1 N. C. Greenham and R. H. Friend, *Solid State Phys.*, 1995, **49**, 1 and references therein.
- 2 A. Kraft, A. C. Grimsdale and A. B. Holmes, *Angew. Chem., Int. Ed.*, 1998, **37**, 402.
- 3 J. H. Burroughes, D. D. C. Bradley, A. R. Brown, R. N. Marks, K. Mackay, R. H. Friend, P. L. Burn and A. B. Holmes, *Nature (London)*, 1990, **347**, 539.
- 4 (a) F. Wudl, P. M. Allemand, G. Srdanov, Z. Ni and D. McBranch, *ACS Symp. Ser.*, 1991, **455**, 683; (b) S. Höger, J. J. McNamara, S. Schriber and F. Wudl, *Chem. Mater.*, 1994, **6**, 171; (c) D.-H. Hwang, S. T. Kim, H.-K. Shim, A. B. Holmes, S. C. Moratti and R. H. Friend, *Chem. Commun.*, 1996, 2241; (d) N. C. Greenham, S. C. Moratti, D. D. C. Bradley, R. H. Friend and A. B. Holmes, *Nature (London)*, 1993, **365**, 628; (e) B. R. Hsieh, Y. Yu, E. W. Forsythe, G. M. Schaaf and W. A. Feld, *J. Am. Chem. Soc.*, 1998, **120**, 231; (f) L. Chiavarone, G. M. Farinola, A. Losacco, M. Striccoli, L. Torsi, G. Scamarcio, M. Sibillano, S. R. Cicco, F. Babudri and F. Naso, *Adv. Sci. Technol. (Faenza, Italy)*, 1999, **27**, 271.
- 5 F. Hide, M. A. Diaz-Garcia, B. J. Schwartz and A. J. Heeger, *Acc. Chem. Res.*, 1997, **30**, 430 and references therein.

- 6 *Electronic Materials: The Oligomer Approach*, ed. K. Müllen and G. Wegner, Wiley-VCH, Weinheim, 1998.
- 7 R. Müller, B. Winkler, F. Stelzer, S. Tasch, C. Hochfilzer and G. Leising, *Synth. Met.*, 1999, **105**, 129.
- 8 H. J. Brouwer, V. V. Krashnikov, T.-A. Pham, R. E. Gil and G. Hadziioannou, *Appl. Phys. Lett.*, 1998, **73**, 708.
- 9 (a) F. Babudri, S. R. Cicco, G. M. Farinola, F. Naso, A. Bolognesi and W. Porzio, *Macromol. Rapid Commun.*, 1996, **17**, 905; (b) F. Babudri, A. R. CiccioMessere, G. M. Farinola, V. Fiandanese, G. Marchese, R. Musio, F. Naso and O. Sciacovelli, *J. Org. Chem.*, 1997, **62**, 3291; (c) F. Babudri, G. M. Farinola, V. Fiandanese, L. Mazzone and F. Naso, *Tetrahedron*, 1998, **54**, 1085; (d) F. Babudri, V. Fiandanese, O. Hassan, A. Punzi and F. Naso, *Tetrahedron*, 1998, **54**, 4327; (e) F. Babudri, A. Cardone, G. M. Farinola and F. Naso, *Tetrahedron*, 1998, **54**, 14609.
- 10 Z. Bao, W. K. Chan and L. Yu, *J. Am. Chem. Soc.*, 1995, **117**, 12426.
- 11 Z. Bao, Y. Chen, R. Cai and L. Yu, *Macromolecules*, 1993, **26**, 5281.
- 12 M. Asakawa, P. R. Ashton, W. Hayes, H. M. Janssen, E. W. Meijer, S. Menzer, D. Pasini, J. Fraser Stoddart, A. J. P. White and D. J. Williams, *J. Am. Chem. Soc.*, 1988, **110**, 920.
- 13 L. Mandolini, B. Masci and S. Roelens, *J. Org. Chem.*, 1977, **42**, 3733.
- 14 O. S. Mills, N. J. Mooney, P. M. Robinson, C. I. F. Watt and B. G. Box, *J. Chem. Soc., Perkin Trans. 2*, 1995, 697.
- 15 V. Francke, T. Mangel and K. Müllen, *Macromolecules*, 1998, **31**, 2447; J. M. Tour, *Chem. Rev.*, 1996, **96**, 537.
- 16 (a) B. Tian, G. Zerbi, R. Schenk and K. Müllen, *J. Chem. Phys.*, 1991, **95**, 3191; (b) H. S. Woo, O. Lhost, S. C. Graham, D. D. C. Bradley, R. H. Friend, C. Quattrocchi, J. L. Brédas, R. Schenk and K. Müllen, *Synth. Met.*, 1993, **59**, 13.
- 17 J. W. Blatchford, S. W. Jessen, L.-B. Lin, T. L. Gustafson, D.-K. Fu, H. -L. Wang, T. M. Swager, A. G. MacDiarmid and A. J. Epstein, *Phys. Rev. B*, 1996, **54**, 9180 and references therein.
- 18 S. V. Frolov, Z. V. Vardeny and K. Yoshino, *Phys. Rev. B*, 1998, **57**, 9141.
- 19 L. Chiavarone, M. Di Terlizzi, G. Scamarcio, G. M. Farinola, F. Babudri and F. Naso, *Appl. Phys. Lett.*, 1999, **75**, 2053.
- 20 I. D. Parker, *J. Appl. Phys.*, 1994, **75**, 1656.
- 21 A. F. Renaldo, J. W. Labadie and J. K. Stille, *Org. Synth.*, 1989, **67**, 86.
- 22 J. De Mello, H. F. Wittmann and R. H. Friend, *Adv. Mater.*, 1997, **9**, 230.
- 23 C. C. Wu, I. Wu, J. C. Sturm and A. Khan, *Appl. Phys. Lett.*, 1997, **70**, 1348.
- 24 N. C. Greenham, I. D. W. Samuel, G. R. Hayes, R. T. Phillips, Y. A. R. R. Kessner, S. C. Moratti, A. B. Holmes and R. H. Friend, *Chem. Phys. Lett.*, 1995, **241**, 89.